JOURNAL OF GEOPHYSICAL RESEARCH, VOL. 89, NO. B6, PAGES 4419-4426, JUNE 10, 1984

THE GRAVSAT SIGNAL OVER TECTONIC FEATURES

C. A. Wagner and D. T. Sandwell

National Geodetic Survey, Charting and Geodetic Services, National Ocean Service
National Oceanic and Atmospheric Administration

Abstract. The range rate between two close gravitational satellites (GRAVSAT) in low earth orbit has been evaluated over model tectonic features such as mountains and ranges, fracture zones, and trenches. Models are locally compensated and consist of both point mass dipoles and sheet mass dipoles. Masses and depths of compensation are chosen to approximate known gravity signatures. The results show that for two satellites at 160 km altitude with 3^{o} separation, significant signal power (>1 μm/s) remains for most extended features at wavelengths less than 200 km. Furthermore, there is strong sensitivity in the signal from these features to lateral and vertical changes of the order of 1 km and less. In addition, the signal of hidden geologic structures such as dikes, salt domes, and ore bodies may also stand above 1 μm/s for this low orbiting pair. Thus, it may prove to be efficient to model the high-frequency GRAVSAT signal directly in terms of the parameters of tectonic-topographic features and their compensation.

Introduction

The advent of precise satellite-satellite tracking contains the promise of more than an order of magnitude improvement in knowledge of the global gravity field [National Research Council, 1979]. Improvement is most needed over many continental areas at subcontinental wavelengths (e.g., in Asia, Africa, and South America) where many geologic and tectonic structures and processes are poorly detected with present data. But improvement is also needed over the oceans (at both long and short wavelengths) to aid in the detection of currents (from satellite altimetry). On the other hand, for the direct purpose of studying in detail the geophysics of the marine crust and lithosphere, current satellite-altimetric geoid data are already proving beneficial [e.g., Brown et al., 1983; Sandwell and Schubert, 1982; McAdoo, 1982; Angevine and Turcotte, 1980]. Undoubtedly, the lack of adequate bathymetry hurts these studies now as much as the altimetric coverage, which needs densification. But anticipating future satellite altimeter missions, we believe the major contribution of improved satellite gravity data will be in continental geophysics.

The satellite mission which promises the most accurate field mapping is known as the low-low gravitational satellite (GRAVSAT) [National Research Council, 1979]. Combined with magnetic mapping, it is now known as the Geopotential Research Mission. By the use of dual two-frequency microwave transmissions, the Doppler shifts between the two drag-compensated satellites are measured to yield a relative range rate between them of better than 1 μm/s for a 4-s averaging time. Numerous studies have concluded that such observations can yield a gravitational field (at sea level) accurate to a few milligals (10^{-2} mm s^{-2}) in mean gravity or about 50 mm in mean geoid anomaly at a resolution length of 1^{o}. [e.g., Jekeli and Rapp, 1980; Douglas et al., 1980]. But the significance of this kind of accuracy on geophysical inference has yet to be examined in any detail. We make a start in this examination by estimating the GRAVSAT signal with respect to a number of model tectonic/geologic features. We also find the sensitivity of that signal to changes in the model parameters. Both of these calculations anticipate the possibility of modeling these features directly from the relative range rate measurements (in conjunction with topographic data). Indeed, a considerable amount of this kind of topographic modeling has already been accomplished with planetary orbiters [e.g., Sjogren, 1974; Sjogren et al., 1980].

Paper number 4B0272.

Models

We wish to compute the effect on a satellite of the complex mass distribution on and near the earth's surface. We want primarily to establish the detectability of various tectonic features. To minimize orbit computations, our initial approach is to determine the forces acting on the satellite from analytic expressions derived from geometrically simple models. Extended discontinuous topography such as continental blocks are expected to show the largest signals. Ideally, these should be modeled as solid spherical prisms (tesseral lamina), but no closed form solution for their attraction exists. On the other hand, complex but analytic expressions of the effect of extended linear features are known, such as the rectangular parallelopiped [Macmillan, 1958, pp. 72-79]. Besides being complex individually, these latter forms must be patched together to fit properly over a spherical earth. Yet if we ignore the central attraction of the earth as a whole and seek just the local effect of the surface feature, we can use these simpler mass representations. In effect, we assume a flat, empty earth as a reference. Later we show the results of two tests of this assumption: (1) with a point mass feature over a spherical solid earth and (2) by comparing the power spectrum of a continental GRAVSAT pass with its expectation for a 'realistic' earth model. Specifically, for large extended structures (fracture zones, ridges, plateaus, trenches, mountain ranges, etc.) we choose combinations of a two dimensional semi-infinite thin slab, locally compensated at depth (Figure 1). The potential and attraction of this discontinuous mass is easily derivable from the logarithmic potential of an infinite rod [e.g., Dorman. 1975; Telford et al.,

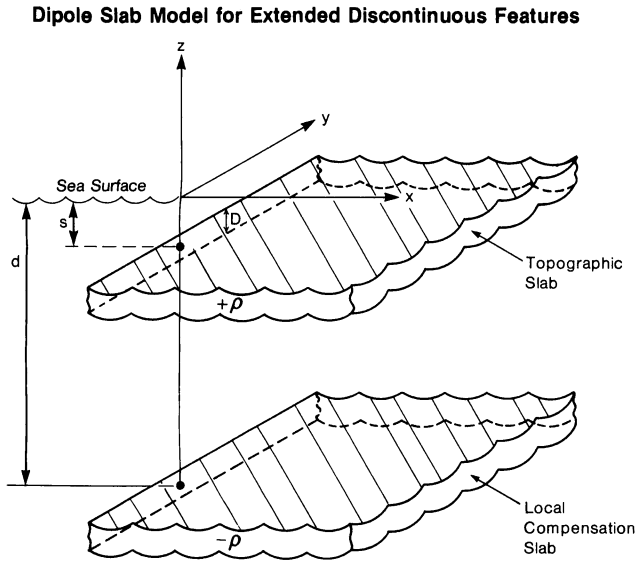

Fig. 1. Dipole slab model for extended discontinuous features. Used for "infinitely" long scarps, plateaus, mountain ranges, trenches, fracture zones, etc. Thickness D must be small compared to height of point above slabs. An infinitely long feature of finite width is estimated by the addition of an inverse dipole slab displaced by that width along the x axis.

1977]. Referring to Figure 1, to obtain the potential, the results for any point x,z away from the slab are [Sandwell and Schubert, 1982, p. 2957]

$$U(x) = 2\pi G\sigma(d+z)\left\{\left[\tfrac{1}{2}\left(1-\frac{s+z}{d+z}\right)+\frac{1}{\pi}\,\mathrm{Tan}^{-1}\left(\frac{x}{d+z}\right)\right.\right.$$

$$\left.\left.-\left(\frac{s+z}{d+z}\right)\mathrm{Tan}^{-1}\left(\frac{x}{s+z}\right)+\frac{x}{2\pi(d+z)}\,\ell n\,\frac{x^2+(d+z)^2}{x^2+(s+z)^2}\right]\right\} \quad (1)$$

where G is the universal gravity constant (6.67 x 10^{-11} nt m^2kg^{-2}), s and d are the depths to the slab and its compensation, and σ is the density contrast of the slab per unit area:

$$\sigma = D\delta\rho$$

$\delta\rho$ being the volume density contrast and D the thickness of the slab material. The attraction is given by

$$F_x = G\sigma\,\ell n\,\frac{x^2+(d+z)^2}{x^2+(s+z)^2} \quad (2)$$

$$F_z = 2G\sigma\left[\mathrm{Tan}^{-1}\frac{x}{(d+z)}-\mathrm{Tan}^{-1}\frac{x}{(s+z)}\right] \quad (3)$$

We have also used the attraction of a finite rod [e.g., Macmillan, 1958, pp. 191-193] to model dikes. To estimate the effects of the two-dimensional approximation, we compared the results for an infinite rod with results for a 1000-km rod. We find from these that for GRAVSAT altitudes of around 200 km there should be no appreciable difference between the given results for a semi-infinite slab and those for a "finite" slab of the same length ($\sim$ 1000 km). The extended portion of the slab has only a small gravitational effect because it is locally compensated.

All other mass modeling was accomplished with point masses (mountains and ore bodies such as salt domes). These features could be easily approximated with only a small number of mass points within a 100-km region.

We used a Runge-Kutta fourth-order integrator to solve the trajectory equations for the pair of satellites. Step size was generally below 5 s to ensure energy invariance to 12 significant figures. Initial horizontal velocities were equivalent to low circular orbit velocity over a "real earth" (e.g., $\sim$ 7.8 km/s).

A satellite separation of 3° (342 km) at an altitude of 160 km was used in all simulations presented here. The altitude is near the limit for a feasible 6-month mission. The separation is a compromise between a number of factors: single-feature sensitivity (see below), signal to noise ratio, and discrimination width between features. A single mass structure yields the strongest signal if the separation is infinite. But the signal to noise ratio (especially considering ionospheric effects) deteriorates markedly at separations greater than about 6° ($\sim$ 800 km). In addition, recent error analyses [e.g., Douglas et al., 1980] appear to confirm the widely held view that the useful discrimination width in a GRAVSAT mission is of the order of the satellite's altitude [e.g., Schwarz, 1972]. But since the measurement is the difference of two perturbations, a single separation distance (for a close pair) incurs the risk of losing discrimination of structures with just that wavelength [e.g., Breakwell, 1979]. Therefore the actual mission will probably employ a number of separations (between 100 and 600 km).

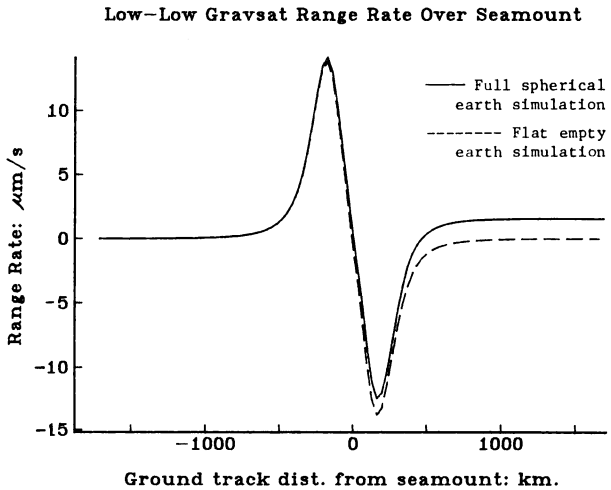

Fig. 2. Low-low GRAVSAT range rate over seamount. The pair approaches from the left at 160 km altitude, 342 km separation (3°), and 7.81 km/s velocity. Distance is with respect to mean of satellite pair. The approach character is the same in all following simulations (except as noted. Seamount cone: base depth, 5 km; width, 50 km; height, 3 km; compensation depth, 20 km; density contrast, 1700 kg m^{-3}.

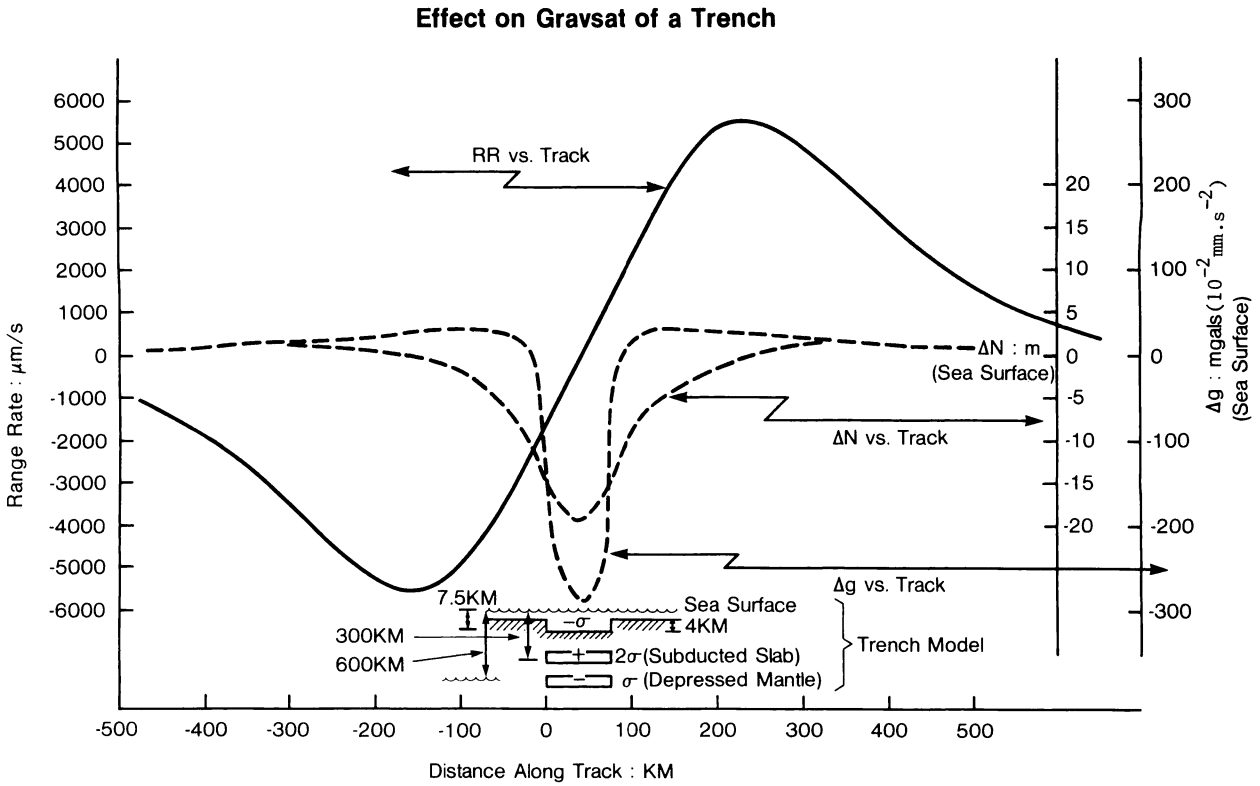

Fig. 3. Effect on GRAVSAT of a trench. The approach is at right angles to the trench axis. Density contrast is 1700 kg m^{-3}.

Results of Simulations

GRAVSAT will probably be most useful for continental geophysics, although we were curious to see if oceanic structures produce detectable signals. Figure 2 shows the relative range rate between two satellites passing directly over a seamount. Referring to Figure 2, the seamount mass point represents a conical figure with a base of 50 km and a height of 3 km sitting on the ocean floor at a depth of 5 km. The "ground track" distance is along the sea surface from the mean of the two satellites to the seamount position. The compensation depth was taken as 20 km, which (together with a density contrast of 1700 kg m^{-3}) yielded a compensated "cone model" anomaly of 110 mgal (1.1 mm s^{-2}) at the sea surface. The point mass dipole seamount had an unrealistically high surface gravity anomaly due to its closeness to the surface. However, at 160 km altitude the anomalies of the compensated cone seamount and the mass point dipole differed by less than 1.6%.

The signal in Figure 2 is typical of concentrated features. Approaching the closer positive mass, the leading spacecraft speeds up. Staddling the feature, the leading spacecraft is pulled back while the trailing one speeds up until a maximum closing relative velocity occurs near the point where the trailing satellite passes the mass concentration. At great distances the relative velocity again approaches zero as the trailing satellite is pulled back, increasing the separation rate.

The maximum signal over the seamount is about 15 μm/s and is greater than the discrimination level for GRAVSAT of 1 μm/s as long as the track approaches to at least 3 1/2° (400 km) from the sea surface position of the mount. Note also from Figure 2 that there is remarkably little difference between the spherical and flat earth simulations. Because the two satellites do not start and end at infinite distance from the mass points, there is a small energy difference between them. This is exaggerated in the spherical case due to the large central force. The final range rate is small in this case but significantly positive.

We have also simulated passes over slightly closer (to GRAVSAT) continental mountains with 100-km bases and smaller heights (1 km) but deeper compensation (45 km) and higher density contrast (2700 kg m^{-3}). The maximum signal is correspondingly larger (75 μm/s).

A truly massive signal (of roughly the same character) is generated by our ocean trench model (Figure 3). This compensation model, proposed by Hager [1983], assumes that about twice the mass deficit in the trench is effective in the cold subducted ocean crust down to a level of about 600 km in the mantle. Hager also estimates that the compensation is only completed when the slab comes to rest, depressing the denser lower mantle. The large amplitude of the range rate signal (Figure 3) is due to both the large mass deficit of the trench and the large distances between compensating bodies (300 km). The deeper masses also act to broaden the effect on GRAVSAT. Figure 3 indicates that with this model both maximum geoid heights and anomalies are quite reasonable ($\sim$ 19 m and 300 mgal (3 mm s^{-2})) for large Pacific trenches.

We expect that a comparison of the GRAVSAT signal (at altitude) with sea surface anomalies

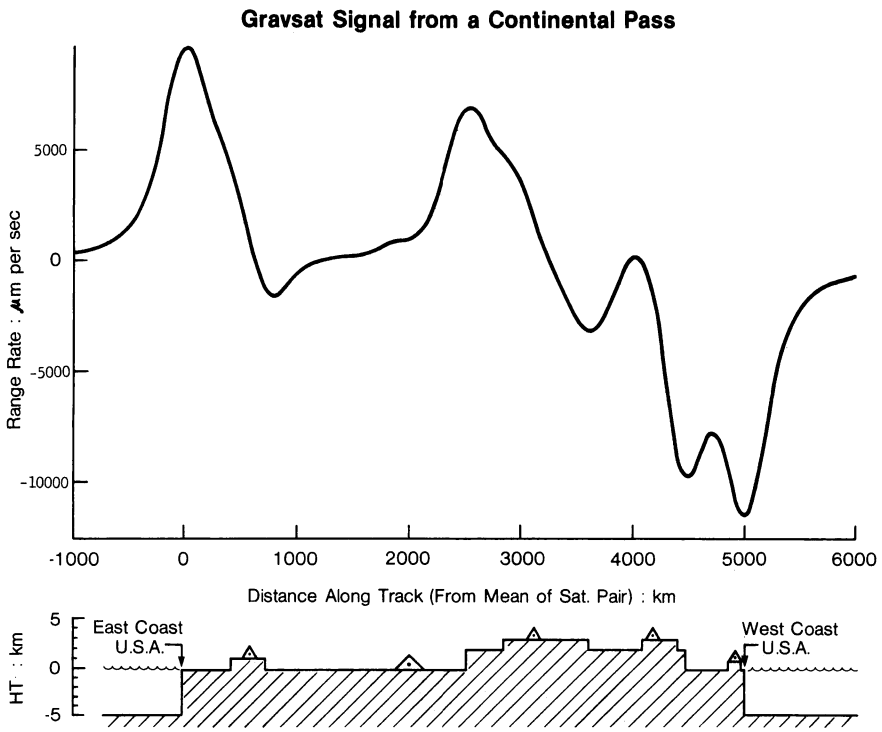

Fig. 4. GRAVSAT signal from a continental pass. Topography is simulated over the United States at about 38°N: Continental craton; density contrast, 1700 kg m^{-3}; Appalachian, Rocky, Sierra Nevada, west coast mountain ranges, western plateau, as shown; individual cone mountains; 100 km widths, 1 km heights as shown except Ozarks, 200 km width; density constrasts, 2700 kg m^{-3}. The approach is at right angles to the axes of extended features.

will be a powerful constraint on the compensation mechanism for trenches (as for other ocean crust features). Recall that Murphy and Siry [1970] were able to show from high and low passes of different lunar orbiters that the moon's buried mass concentrations were probably at shallow depth. The combination of GRAVSAT tracking and sea surface anomaly (gravity or geoid) data should yield similar information. Later we show specifically the strong sensitivity of the GRAVSAT signal to compensation depth alone.

Figure 4 shows the GRAVSAT signal of a pass over a model continent made to simulate the United States at about 38°N [Sloss and Heirtzler, 1982]. The signal is dominated by the broad edge effects of the continental margins (5-km 'step') and the western plateau (2-km step). Also seen clearly are the 1-km steps of the mountain chains: the Rockies (700 km wide), the Sierras (300 km wide), and the Appalachians (300 km wide).

The only other feature which is clearly visible in the signal is the Ozark mountains, which are modeled as a single point mass representing a cone 1 km high with a base 200 km wide. The effects of the west coast range are mostly absorbed by the adjacent continental margin.

To validate the mass model of the continent, we have compared the gravity anomalies computed from it with continental 1° x 1° anomaly data continued upward to 160 km altitude (Figure 5). The model anomalies are generally more energetic but otherwise conform fairly well to those predicted from surface measurements. The one serious discrepancy is that the Sierra Nevada does not appear to show in the upward continued data. But we may have overemphasized the mass of this range. Certainly, it is more a finite wedge than a full infinitely long block. (In addition, the effective compensation depth for the Sierras may be shallower than 45 km). Nevertheless, the comparison appears adequate for a preliminary study.

As a further check of the modeling we have also compared (Figure 6) the range rate power spectrum in this pass to that expected on a similar arc of GRAVSAT over a spherical earth with a potential following "Kaula's rule" [Kaula, 1966]. The expected power in Figure 6 was estimated from a signal computed with harmonics only to degree 180 [Wagner, 1983]. Beyond a frequency of about 140 cycles/revolution these data are mostly extrapolated. However, the overall comparison is good. Note especially the loss of power near 120 cycles, which is expected since the satellite pair is about 3° apart.

We have also computed the signal over smaller linear and dome features whose mass is relatively uncompensated or regionally compensated. For example, a centered pass perpendicular to the axis of a 100 km uncompensated dike (300 kg m^{-3} density contrast) of 500 m width and 10 km thickness yields a maximum relative range rate of 4.5 μm/s. Similarly, a pass over a salt dome treated as a buried spherical body of 4 km radius (200 kg m^{-3} contrast) yielding a surface anomaly of 10 mgal (0.1 mm s^{-2}) produces a maximum signal on GRAVSAT of 1.5 μm/s. Both of these structures [e.g., Whitten and Brooks, 1972; Turcotte and Schubert, 1982] certainly distort their surroundings in such a way as to reduce the anomalous signal. However, because the loads are relatively small, the compensation is regional, and the signal reduction is probably minor.

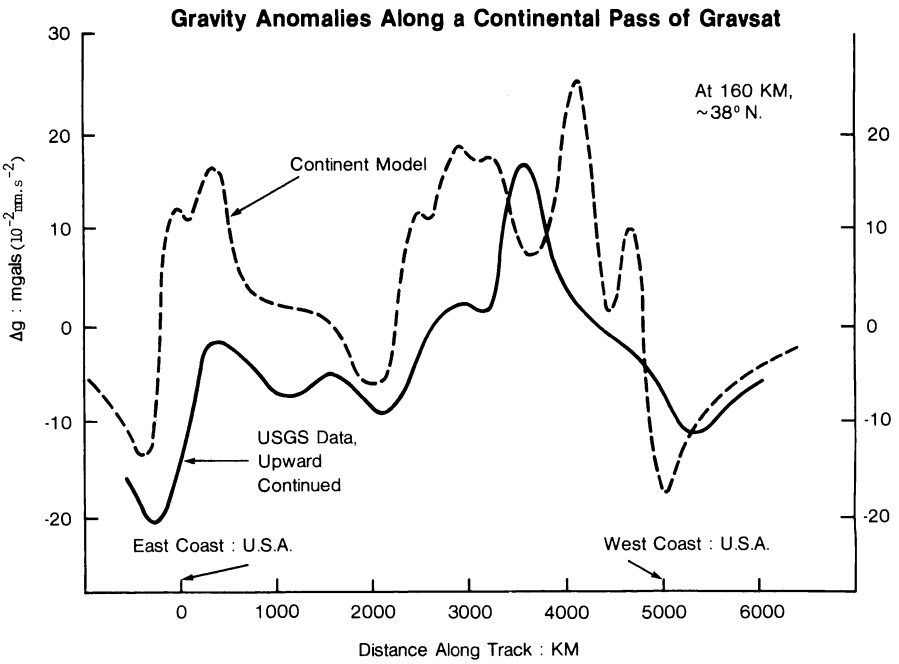

Fig. 5. Gravity anomalies along a continental pass of GRAVSAT. Upward continued data are as computed from 1° x 1° anomalies by J. Phillips (U.S. Geological Survey, 1983).

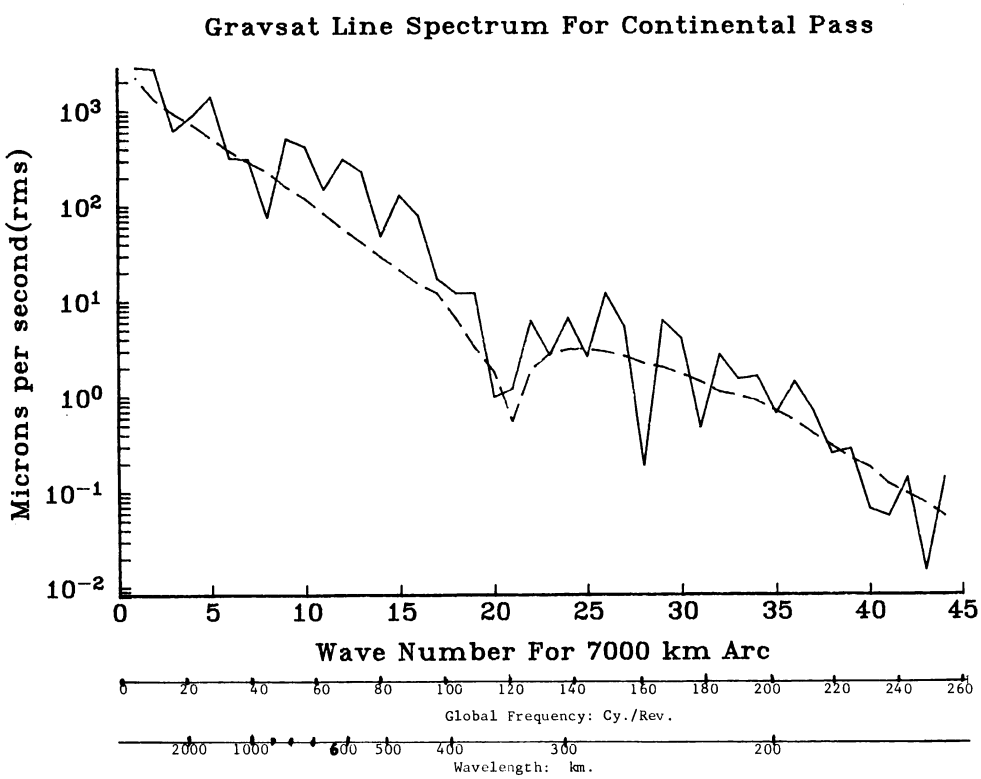

Fig. 6. GRAVSAT line spectrum for continental pass. Solid curve: computed spectrum at discrete wave numbers. Dashed curve: estimated spectrum for polar-orbiting GRAVSAT pair (3° separation, 160 km altitude). Original estimated data, power (rms) in 1 cycle/revolution frequency spans. Kaula's rule was used for geopotential. Power (rms) was estimated for arc wave numbers as rss of "global" power over appropriate (41,079 km/7000 km) cycle/revolution spans.

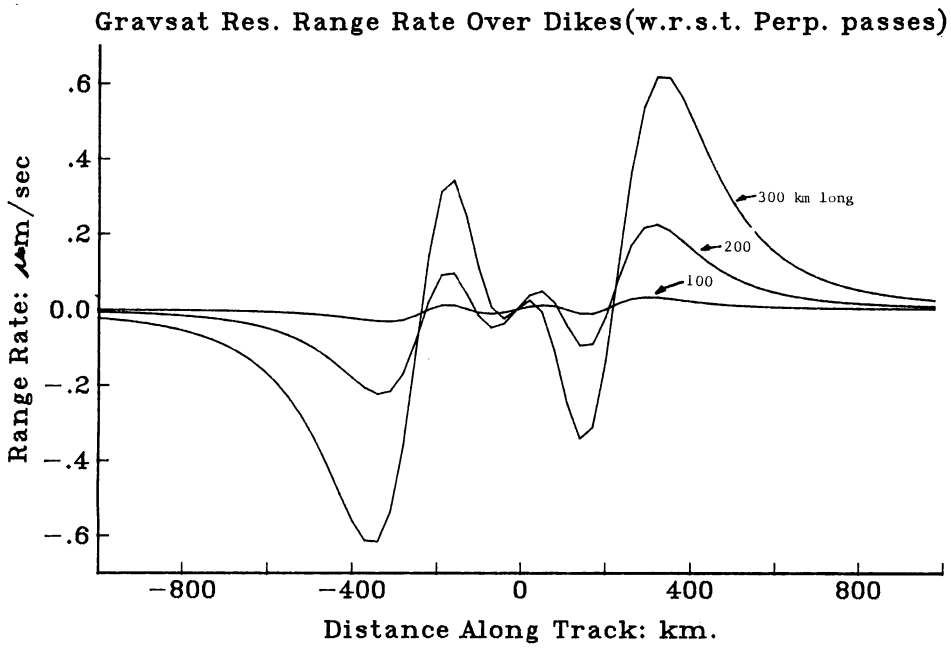

Fig. 7. GRAVSAT residual range rate over dikes with respect to perpendicular passes. The residual curves show the differences (collinear minus centered perpendicular) for passes over dikes (all 500 m wide, 300 kg m^{-3} density contrast) of 100, 200, and 300 km length. The center of the dike is at zero distance along track.

Sensitivity to Tectonic Parameters

With range rate sensitivity at the submicron per second level, GRAVSAT will provide information on the orientation of small continuous structures. For a finite linear mass such as a dike, the structure is sensed as a multiple body for (colinear) passes along the axis. For passes perpendicular to the axis the attraction is much closer to that of a fixed mass. For example, Figure 7 shows the difference in the range rate between centered perpendicular and axial passes of GRAVSAT over dikes of various lengths.

How sensitive is the signal to small changes in the parameters for other structures? Extended features such as mountain ranges and fracture zones will show large changes in range rate for small vertical or horizontal shifts of topography or compensation. For example, a 100-km-wide mountain range (1-km high) shows a 17-μm/s maximum residual signal for a 1-km shift of compensation depth (45-km reference depth). The residual signature is similar to that of the familiar mass concentration (e.g., Figure 2) because it merely represents the effects of a 1-km separated dipole slab at compensation depths. But the sense of the signature distinguishes between too deep or too shallow compensation in the model. Thus if the residual (true minus modeled) rate rises as the feature is approached, then the model depth is too small. If it falls, the depth is too great.

On the other hand, a mountain misplaced horizontally by only 1 km yields a different residual signal shown in Figure 8. Here again the mountain has been modeled as a point mass dipole. But the residual is now due to the combination of the familiar response with its horizontally shifted inverse. The effect of this small double dipole is only visible at the submicron level. But similar residuals for large extended features are significant and also reveal (in their sense) the direction of model shift. Figure 9, for example, shows the residual signal in the continental pass with respect to the same terrain model shifted east horizontally by only 1 km (compare with Figure 4).

The sensitivity is much better with respect to discriminating parts of mountain massifs at a 50-km rather than 1-km scale. Figure 10 shows the residuals to a configuration of five small (point) mountain masses making up 50 km x 50 km x 0.5 km parts of a 100 km x 100 km x 1 km massif block. A single reference mass for the whole block was taken at its center. The residuals

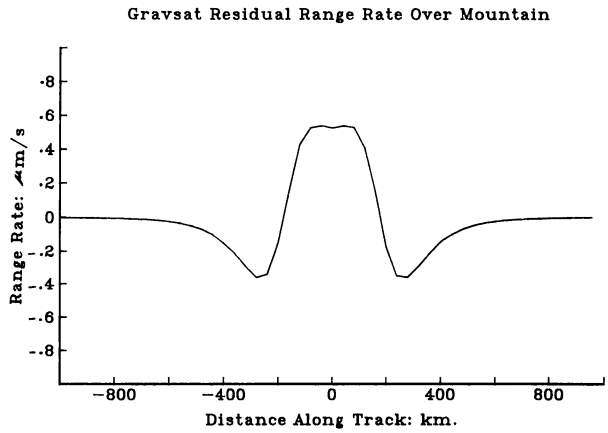

Fig. 8. GRAVSAT residual range rate over mountain. The signal is the difference of two passes over a "cone" mountain 50 km wide and 1 km high (compensated at 45 km depth), with the base at sea level. The mountain in the second pass is shifted left by 1 km. Density contrast is 2700 kg m^{-3}.

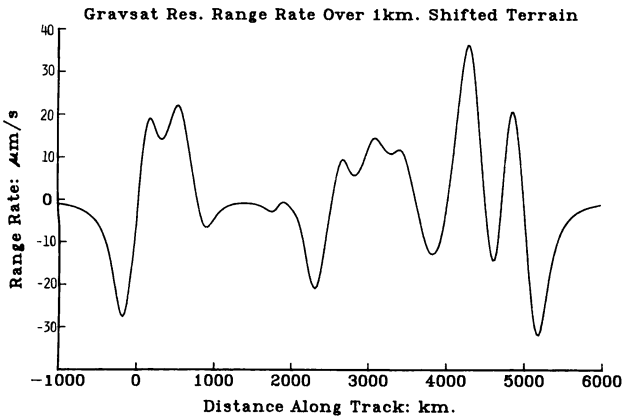

Fig. 9. GRAVSAT residual range rate with respect to 1 km east shifted terrain in a continental pass. The observed range rates are the same as in Figure 4.

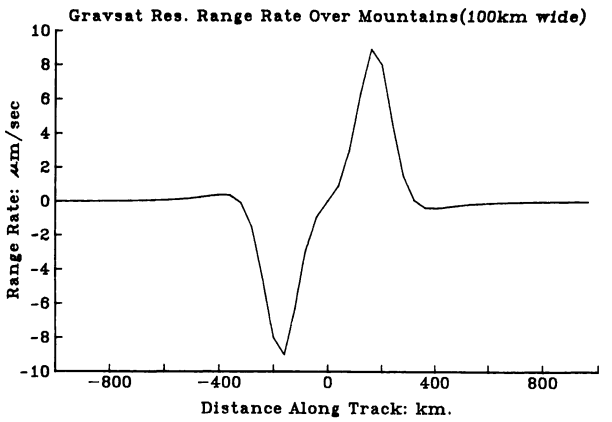

Fig. 10. GRAVSAT residual range rate over mountains (100 km wide). The signal is the difference of two passes over a mountain complex. Detailed model: five point masses representing 50 km x 50 km x 0.5 km blocks (four in a 100 km x 100 km square at sea level, one at 0.5 km altitude, both levels centered at 0 km along track). The reference model is a single point mass at the center of gravity of the complex. Compensation depth is 45 km.

clearly show the separate effects of the leading and lagging 50-km subblocks.

This last simulation indicates that there is considerable information in the GRAVSAT signal to aid in discriminating structures at the 50 x 50 km ($1/2^{o}$ x $1/2^{o}$) level. Another way to gauge the sensitivity to these finer structures is through the power spectrum. Figure 6 shows some response at levels over 1 μm/s for frequencies above 180 cycles/revolution in the GRAVSAT continental pass. Only geopotential harmonics of degree greater than 180 (due to structures finer than 1^{o} x 1^{o}) can be responsible for these frequencies. We can also estimate this fine structure signal directly by evaluating only the attraction of the residual potential along the continental pass. Figure 11 shows this residual signal for that potential above degree 180 found from harmonic analysis. As can be inferred from Figure 6, it is indeed dominated by frequencies close to 220 km wavelength. It shows little detail beyond that due to rapid attenuation of higher harmonics, but the maximum signal is over 4 μm/s.

Discussion

The purpose of this study was to explore the possibility of modeling surface/tectonic features directly from low-low GRAVSAT data. Though the simulations appear reasonable, they are highly simplified. In practice we would model the extended features by tesseral lamina over a spherical earth [Morrison, 1980]. The reference gravity field would not be zero (as here!) but of some low degree (perhaps 8) to account sufficiently for deep mantle anomalies not closely associated with surface structures. Thus we would first have to remove the effects on this reference field of the reference surface masses. The full effects of orbit parameter adjustment to the actual intersatellite GRAVSAT data would also have to be accounted. But this type of efficient simulation-modeling has already been successful with much cruder range rate data to lunar, Martian, and Venus orbiters [e.g., Sjogren, 1974; Sjogren et al., 1980]. At 1 μm/s resolution an earth-orbiting GRAVSAT at 160 km altitude should show more near-surface detail than these.

Note also that upward continuation of the field reduces contrast as well as signal. Thus the actual discrimination of small features (e.g., mountains, domes, dikes) from the much larger background of extended masses (e.g., mountain ranges, trenches, fracture zones) will undoubtedly require a good physical description of the extended features in the reference model. Physiographic maps can supply much of this information. But it may be that fine detail will only be well resolved when a global 1^{o} or 2^{o} reference field is first produced from the range rate data. The fine structure could then be determined by analysis of residuals to this global model. In either case the use of surface/tectonic parameters directly should prove beneficial.

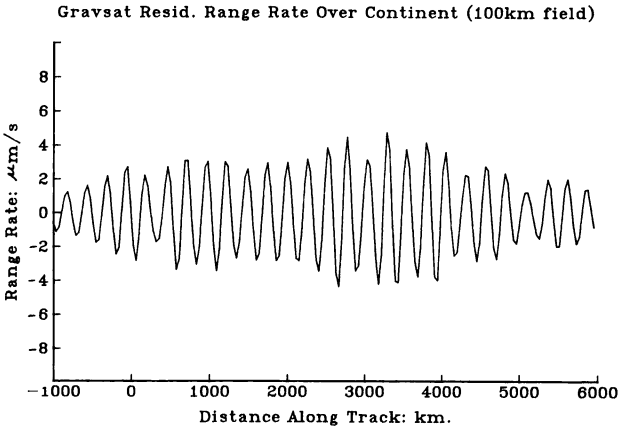

Fig. 11. GRAVSAT ("high pass") residual range rate over continent (100-km field). The signal is the difference of the effects of a full field (Figure 4) and the effects of a "low degree" field representing the potential in this model to a resolution limit of 100 km. Note that the western side of the continent is somewhat more energetic than the east at these short wavelengths.

Conclusions

Simulations show that many kinds of extended and concentrated mass features, compensated and uncompensated, should have significant signals on a low-low GRAVSAT at 160 km altitude. Sensitivity studies also reveal that geophysically interesting parameters of these features (e.g., compensation depth and horizontal location) should be strongly constrained by GRAVSAT data (though not uniquely determined by them). Results also show that some significant signal will be present due to near surface structures less than $1^{\circ} \times 1^{\circ}$ in extent.

Previous analysis of planetary orbiter range rates have already demonstrated the ease with which surface mass features can be directly modeled.

Over continents where topography is well known, but detailed gravity not, direct determination of mass compensation depth for these surface features should be feasible. Over the oceans where bathymetry data are poor but geoid data are plentiful (from satellite altimetry), both bottom topography and its compensation could also be inferred by combining the two levels of data (geoid plus GRAVSAT). Where bathymetry is adequate, this combination will provide additional constraints on deeper (more complex) compensation mechanisms (e.g., in subduction zones).

Acknowledgments. We thank Peter Bender of the Joint Institute for Laboratory Astrophysics of the National Bureau of Standards and the University of Colorado for his interest in this work and for suggesting some of the sensitivity analyses. We also thank James Marsh, a reviewer, for thoughtful comments.

References

Angevine, C. L., and D. L. Turcotte, On the compensation mechanism of the Walvis Ridge, Geophys. Res. Letters 7, 447-479, 1980.

Breakwell, J., Satellite determination of short wavelength gravity variations, J. Astronaut. Sci., 27 (4), 329-344, 1979.

Brown, R. D., W. D. Kahn, D. C. McAdoo and W. E. Himwich, Roughness of the marine geoid from Seasat altimetry, J. Geophys. Res., 88, 1531-1540, 1983.

Dorman, L. M., The gravitational edge effect, J. Geophys. Res., 80, 2949-2950, 1975.

Douglas, B. C., C. C. Goad, and F. Morrison, Determination of the geopotential from satellite-to-satellite tracking data, J. Geophys. Res., 85, 5471-5480, 1980.

Hager, B. H., Subducted slabs and the geoid: Constraints on mantle rheology and flow, Seismol. Lab. Rep. 252-21 Calif. Inst. of Technol., Pasadena, 1983.

Jekeli, C., and R. H. Rapp, Accuracy of the determination of mean anomalies and mean geoid undulations from a satellite gravity field mapping mission, Dept. of Geod. Sci., Rep. 307, Ohio State Univ., Columbus, 1980.

Kaula, W. M., Satellite Geodesy, p. 98, Blaisdell, Waltham, Mass., 1966.

Macmillan, W. D., Theory of the Potential, Dover, New York, 1958.

McAdoo, D. C., On the compensation of geoid anomalies due to subducting slabs, J. Geophys. Res., 87, 8684-8692, 1982.

Morrison, F., Computing the potential and attraction of a density layer by means of elliptic integrals, Manuscr. Geod., 5, 145-173, 1980.

Murphy, J., and J. Siry, Lunar mascon evidence from apollo orbits, Planet. Space Sci., 18, 1137-1141, 1970.

National Research Council, Applications of a dedicated gravitational satellite mission, report, Nat. Acad. of Sci., Washington, D.C., 1979.

Sandwell, D. T., and G. Schubert, Geoid height-age relation from Seasat altimeter profiles across the Mendocino Fracture Zone, J. Geophys. Res., 87, 3949-3958, 1982.

Schwarz, C. R., Refinement of the gravity field by satellite-to-satellite Doppler tracking, in The Use of Artificial Satellites for Geodesy, Geophys. Monogr. Ser., vol. 15, edited by S. W. Henriksen et al., pp. 133-138, AGU, Washington, D.C., 1972.

Sjogren, W. L., Lunar satellite techniques applicable to earth satellite geodesy, in The Use of Artificial Satellites for Geodesy and Geodynamics, pp. 449-467, National Technical University of Athens, Greece, 1974.

Sjogren, W. L., R. J. Phillips, P. W. Birkeland, and R. N. Wimberly, Gravity anomalies on Venus, J. Geophys. Res., 85, 8300-8302, 1980.

Sloss, P. W., and J. R. Heirtzler, Cover, Eos Trans. AGU, 63 (37), 784, 1982.

Telford, W. M., L. P. Geldart, R. E. Sheriff, and D. A. Keys, Applied Physics, pp. 10-11, Cambridge University Press, New York, 1977.

Turcotte, D. L., and G. Schubert, Geodynamics: Applications of Continuum Physics to Geological Problems, pp. 212-214, John Wiley, New York, 1982.

Wagner, C. A., Direct determination of gravitational harmonics from GRAVSAT data, J. Geophys. Res. 88, 10309-10321, 1983.

Whitten, D. G. A., and J. R. V. Brooks, A Dictionary of Geology, pp. 136-138, Penguin Books, New York, 1972.

D. T. Sandwell and C. A. Wagner, National Geodetic Survey, Charting and Geodetic Services, NOS/NOAA, Rockville, MD 20852.

(Received October 11, 1983;
revised February 13, 1984;
accepted February 14, 1984.)